

## K<sup>-</sup> multi-nucleon absorption processes in hadronic interaction studies

R. Del Grande<sup>\*ab</sup>

M. Cargnelli<sup>c</sup>, C. Curceanu<sup>a</sup>, L. Fabbietti<sup>d</sup>, J. Marton<sup>c</sup>, K. Piscicchia<sup>ae</sup>, A. Scordo<sup>a</sup>,  
D. Sirghi<sup>af</sup>, I. Tucakovic<sup>g</sup>, O. Vazquez Doce<sup>d</sup>, S. Wycech<sup>h</sup>, J. Zmeskal<sup>c</sup>,  
A. Anastasi<sup>ai</sup>, F. Curciarello<sup>ijk</sup>, E. Czerwinski<sup>l</sup>, W. Krzemien<sup>h</sup>, G. Mandaglio<sup>im</sup>,  
M. Martini<sup>an</sup>, P. Moskal<sup>l</sup>, V. Patera<sup>op</sup>, E. Perez del Rio<sup>a</sup>, M. Silarski<sup>a</sup>

on behalf of the AMADEUS collaboration.

<sup>a</sup> INFN Laboratori Nazionali di Frascati, Frascati, Italy.

<sup>b</sup> Dipartimento di Fisica, Università degli Studi di Roma Tor Vergata, Roma, Italy.

<sup>c</sup> Stefan-Meyer-Institut für Subatomare Physik, Wien, Austria.

<sup>d</sup> Excellence Cluster Universe, Technische Universität München, Garching, Germany.

<sup>e</sup> Museo Storico della Fisica e Centro Studi e Ricerche "Enrico Fermi", Roma, Italy.

<sup>f</sup> Horia Hulubei National Institute of Physics and Nuclear Engineering (IFIN-HH), Magurele, Romania.

<sup>g</sup> Ruđer Bošković Institute, Zagreb, Croatia.

<sup>h</sup> National Centre for Nuclear Research, Warsaw, Poland.

<sup>i</sup> Dipartimento M.I.F.T. dell'Università di Messina, Messina, Italy.

<sup>j</sup> Novosibirsk State University, Novosibirsk, Russia.

<sup>k</sup> INFN Sezione Catania, Catania, Italy.

<sup>l</sup> Institute of Physics, Jagiellonian University, Cracow, Poland.

<sup>m</sup> INFN Gruppo collegato di Messina, Messina, Italy.

<sup>n</sup> Dipartimento di Scienze e Tecnologie applicate, Università "Guglielmo Marconi", Roma, Italy.

<sup>o</sup> Dipartimento di Scienze di Base e Applicate per l'Ingegneria, Sapienza Università di Roma, Roma, Italy.

<sup>p</sup> INFN Sezione di Roma, Roma, Italy.

E-mail: [raffaele.delgrande@lnf.infn.it](mailto:raffaele.delgrande@lnf.infn.it)

The AMADEUS collaboration aims to afford unprecedented informations on the K<sup>-</sup> low-energy interactions with light nuclei, thanks to the unique monochromatic low-momentum kaons provided by the DAΦNE collider and the excellent acceptance and resolution of the KLOE detector, used as an active target. We will report on the measurement of the yield of the K<sup>-</sup> two nucleon absorption process, obtained by studying Σ<sup>0</sup>p pairs produced in the final state of the K<sup>-</sup> <sup>12</sup>C absorptions. Further, the possible contribution of a ppK<sup>-</sup> bound state was investigated. The best fit gives space to a yield of  $ppK^-/K_{stop}^- = (0.044 \pm 0.009 \text{ stat}_{-0.005}^{+0.004} \text{ syst}) \times 10^{-2}$  corresponding to a binding energy and a width of 45 and 30 MeV/c<sup>2</sup>, respectively. A statistical analysis of this result shows although that its significance is only at the level of 1σ.

54th International Winter Meeting on Nuclear Physics

25-29 January 2016

Bormio, Italy

## 1. Introduction

The AMADEUS collaboration [1] [2] study the low-energy K<sup>-</sup> interactions with light nuclei (H, <sup>4</sup>He, <sup>9</sup>Be and <sup>12</sup>C), with the aim to explore the non-perturbative QCD regime in the strangeness sector. The AMADEUS program focuses in particular on the quantitative investigation of the  $\bar{K}$  nucleon and multi-nucleon interactions strength, of crucial importance in various sectors of physics, ranging from nuclear physics to astrophysics, where strangeness and hyperons formation could play a role in the Equation of State (EoS) of Neutron Stars [3]. The strength of the  $\bar{K}N$  potential influences the parameters of the controversial  $\Lambda(1405)$  state [4], being also related to the possible formation of the so-called kaonic bound states [5] [6], in which one or more nucleons could be kept together by the strong attractive interaction with antikaons. Objects like ppK<sup>-</sup> or ppnK<sup>-</sup> might then be formed. From the experimental point of view two main approaches have been used for studying the ppK<sup>-</sup> cluster: p-p collisions [7] [8], and in-flight or stopped K<sup>-</sup> interactions in light nuclei. For the second, results have been published by the FINUDA [9] and KEK-PS E549 collaborations [10] through the investigation of the  $\Lambda p$  final state. The interpretation of these results is far from being conclusive, and it requires an accurate description of the single and multi-nucleon absorption processes that a K<sup>-</sup> would undergo when interacting with light nuclei. AMADEUS takes advantage of the DAΦNE collider at the LNF-INFN in Frascati, which provides a unique source of monochromatic low-momentum kaons and exploits the KLOE detector as an active target, in order to obtain excellent acceptance and resolution data for the K<sup>-</sup> nuclear capture, both at-rest and in-flight. From the analysis of the KLOE 2004-2005 data set, both the strength of the K<sup>-</sup> binding in nuclei and the  $\Sigma(1385)$  and  $\Lambda(1405)$  resonances properties can be extracted by analysing, respectively, the  $\Lambda/\Sigma$ -p,d,t channels and the decay channels  $\Lambda/\Sigma - \pi$ . This paper focuses, in particular, on the study of the  $\Sigma^0 p$  final state produced in absorption processes of K<sup>-</sup> on two or more nucleons, occurring in the KLOE Drift Chamber (DC) entrance wall which is composed by solid carbon, and on the search for a signature of the ppK<sup>-</sup> →  $\Sigma^0 + p$  kaonic bound state. A more detailed description of the analysis procedures can be found in [11].

## 2. The DAΦNE collider and the KLOE detector

DAΦNE [12] (Double Anular  $\Phi$ -factory for Nice Experiments) is a double ring  $e^+ e^-$  collider, designed to work at the center-of-mass energy of the  $\phi$  particle  $m_\phi = (1019.456 \pm 0.020)$  MeV/c<sup>2</sup>. The  $\phi$  meson decay produces charged kaons (with BR(K<sup>+</sup> K<sup>-</sup>) = 48.9 ± 0.5%) with low momentum (~ 127 MeV/c) which is ideal either to stop them, or to explore the products of the low-energy nuclear absorptions of K<sup>-</sup>s. The KLOE detector [13] is centered around the interaction region of DAΦNE and is characterised by a  $\sim 4\pi$  geometry and an acceptance of  $\sim 98\%$ ; it consists of a large cylindrical Drift Chamber (DC) and a fine sampling lead-scintillating fibers calorimeter, all immersed in an axial magnetic field of 0.52 T, provided by a superconducting solenoid. The DC [14] has an inner radius of 0.25 m, an outer radius of 2 m and a length of 3.3 m. The DC entrance wall composition is 750 μm of carbon fibre and 150 μm of aluminium foil. Dedicated GEANT MonteCarlo simulations of the KLOE apparatus were performed to estimate the percentages of K<sup>-</sup> absorptions in the materials of the DC entrance wall (the K<sup>-</sup> absorption physics were treated

---

\*Speaker.

by the GEISHA package). Out of the total number of kaons interacting in the DC entrance wall, about 81% results to be absorbed in the carbon fibre component and the residual 19% in the aluminium foil. The KLOE DC is filled with a mixture of helium and isobutane (90% in volume <sup>4</sup>He and 10% in volume C<sub>4</sub>H<sub>10</sub>) and is characterised by excellent position and momentum resolutions. Tracks are reconstructed with a resolution in the transverse  $R - \phi$  plane of  $\sigma_{R\phi} \sim 200 \mu\text{m}$  and a resolution along the z-axis of  $\sigma_z \sim 2 \text{mm}$ . The transverse momentum resolution for low momentum tracks ( $(50 < p < 300) \text{ MeV}/c$ ) is  $\frac{\sigma_{pT}}{pT} \sim 0.4\%$ . The KLOE calorimeter [15] is composed of a cylindrical barrel and two endcaps, providing a solid angle coverage of 98%. The volume ratio (lead/fibres/glue=42:48:10) is optimised for a high light yield and a high efficiency for photons in the range (20-300) MeV/c. The position of the cluster along the fibres can be obtained with a resolution  $\sigma_{\parallel} \sim 1.4 \text{ cm}/\sqrt{E(\text{GeV})}$ . The resolution in the orthogonal direction is  $\sigma_{\perp} \sim 1.3 \text{ cm}$ . The energy and time resolutions for photon clusters are given by  $\frac{\sigma_E}{E_\gamma} = \frac{0.057}{\sqrt{E_\gamma(\text{GeV})}}$  and  $\sigma_t = \frac{54 \text{ ps}}{\sqrt{E_\gamma(\text{GeV})}}$ . The AMADEUS step 0 consists in the 2004-2005 KLOE collected data analysis, that corresponds to a total integrated luminosity of  $1.74 \text{ fb}^{-1}$ , for which the  $dE/dx$  information of the reconstructed tracks is available ( $dE/dx$  represents the truncated mean of the ADC collected counts due to the ionisation in the DC gas). An important contribution of in-flight K<sup>-</sup> nuclear captures, in different nuclear targets from the KLOE materials, was evidenced and characterised, enabling to perform invariant mass spectroscopy of in-flight K<sup>-</sup> nuclear captures [16].

### 3. The $\Lambda(1116)$ selection

The presence of a hyperon always represents the signature of a K<sup>-</sup> hadronic interaction inside the KLOE setup materials. Most of the analyses introduced in at the beginning then start with the identification of a  $\Lambda(1116)$ , through the reconstruction of the  $\Lambda \rightarrow p + \pi^-$  ( $\text{BR} = 63.9 \pm 0.5\%$ ) decay vertex. In figure 1 left the  $dE/dx$  versus momentum scatterplot for the finally selected protons is shown, where the function used for the selection of protons is displayed in red. The typical signature of pions in  $dE/dx$  versus momentum can be also seen in figure 1 left illustrating the efficient rejection of  $\pi^+$  contamination in a broad range of momentum. A minimum track length of 30 cm is required, and a common vertex is searched for all the  $p-\pi^-$  pairs in each event. When found, the common vertex position is added as an additional constraint for the track refitting. The module of the momentum and the vector cosines are redefined for both tracks, taking into account for the energy loss in the gas and the various crossed materials (signal and field wires, DC wall, beam pipe) when tracks are extrapolated back through the detector. As a final step for the identification of  $\Lambda$  decays, the vertices are cross-checked with quality cuts using the minimum distance between tracks (minimum distance  $< 3.2 \text{ cm}$ ) and the chi-square of the vertex fit. A spatial resolution below 1 mm is achieved for vertices found inside the DC volume (evaluated with Monte Carlo). The invariant mass  $M_{p\pi^-}$ , calculated under the  $p$  and  $\pi^-$  mass hypothesis, is shown in figure 1 right. The Gaussian fit gives a mass of  $1115.723 \pm 0.003 \text{ MeV}/c^2$  and an excellent resolution ( $\sigma$ ) of  $0.3 \text{ MeV}/c^2$ , confirming the unique performances of KLOE for charged particles (the systematics, depending on the momentum calibration of the KLOE setup, are presently under evaluation).

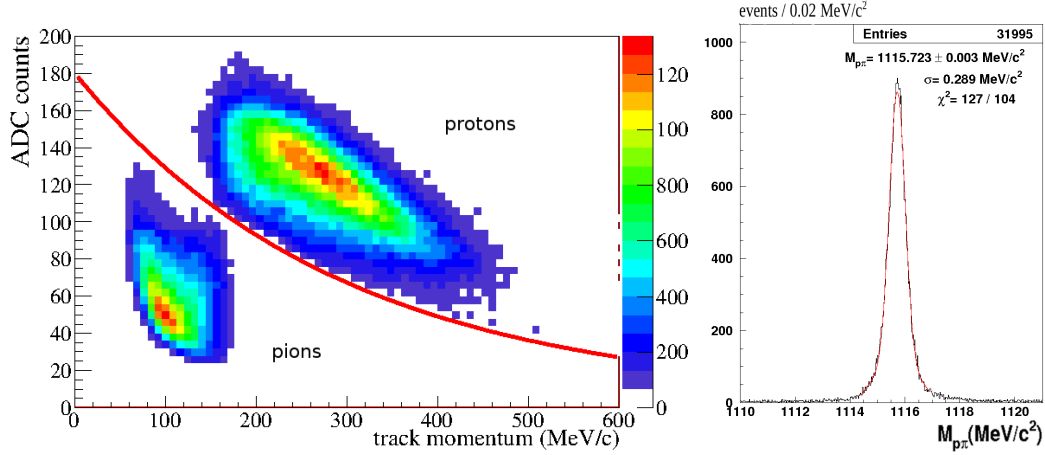


**Figure 1:** Left:  $dE/dx$  (in ADC counts) vs. momentum for the selected proton (up) and pion (down) tracks in the final selection. The proton selection function is displayed in red. Right:  $M_{p\pi^-}$  invariant mass spectrum for the selected pion-proton pairs.

#### 4. $\Sigma^0 p$ analysis

After the  $\Lambda$  search, a common vertex between the  $\Lambda$  candidate and an additional proton track is searched for. The obtained resolution on the radial coordinate for the  $\Lambda p$  vertex is 12 mm, while its invariant mass resolution is found to be, from MC studies, equal to  $1.1 \text{ MeV}/c^2$ . The  $\Sigma^0$  candidates are identified through their decay into  $\Lambda\gamma$  pairs. After the reconstruction of a  $\Lambda p$  pair, the photon selection is carried out via its identification in the EMC. More details are given in [11]. Then, the  $\Sigma^0 p$  invariant mass, opening angle, and the individual  $\Sigma^0$  and proton momenta distributions are considered simultaneously in a global fit to extract the contributions of the various absorption processes. The processes that are taken into account in the fit of the experimental data are:

- $K^- A \rightarrow \Sigma^0 - (\pi) p_{spec}(A')$
- $K^- pp \rightarrow \Sigma^0 - p$  (2NA)
- $K^- ppn \rightarrow \Sigma^0 - p - n$  (3NA)
- $K^- ppnn \rightarrow \Sigma^0 - p - n - n$  (4NA)

where  $A$  is the atomic number of the target nucleus,  $p_{spec}$  is the spectator proton,  $A'$  is the atomic number of the residual nucleus and 2/3/4NA stands for 2/3/4-nucleons absorption. This list includes the  $K^-$  absorption on two nucleons with and without final state interaction (FSI) for the  $\Sigma^0 p$  state and processes involving more than two nucleons in the initial state. These contributions are either extracted from experimental data samples or modelled via simulations. Two kinds of background contribute to the analysed  $\Sigma^0 p$  final state: the machine background and the events with  $\Lambda\pi^0 p$  in the final state. Both are quantified using experimental data [11]. The obtained fit is shown in figure 2 and the results are summarised in table 4.

The final fit results deliver the contributions of the different channels to the analysed  $\Sigma^0 p$  final state. The best fit delivers a reduced chi-square of 0.85. The emission rates extracted from the fit are

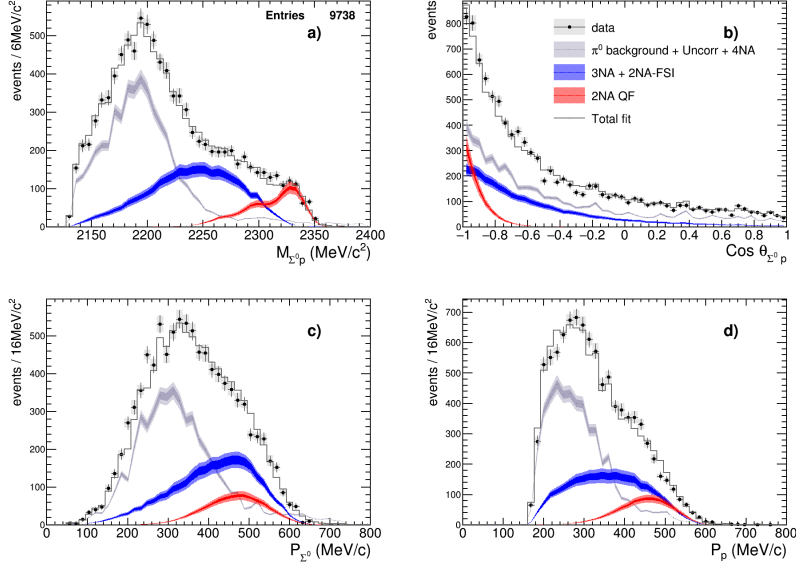


**Figure 2:** Experimental distributions of the  $\Sigma^0 p$  invariant mass,  $\cos(\theta_{\Sigma^0 p})$ ,  $\Sigma^0$  and proton momentum together with the results of the global fit. The experimental data after the subtraction of the machine background are shown by the black circles, the systematic errors are represented by the boxes and the coloured histograms correspond to the fitted signal distributions where the light-coloured bands show the fit errors and the darker bands represent the symmetrised systematic errors. The gray line show the total fit distributions (see [11] for details).

Process	yield / $K_{stop}^- \times 10^{-2}$	$\sigma_{stat} \times 10^{-2}$	$\sigma_{syst} \times 10^{-2}$
2NA-QF	0.127	$\pm 0.019$	+0.004 -0.008
2NA-FSI	0.272	$\pm 0.028$	+0.022 -0.023
Tot 2NA	0.399	$\pm 0.033$	+0.023 -0.032
3NA	0.274	$\pm 0.069$	+0.044 -0.021
Tot 3 body	0.546	$\pm 0.074$	+0.048 -0.033
4NA + bkg.	0.773	$\pm 0.053$	+0.025 -0.076

**Table 1:** Production probability of the  $\Sigma^0 p$  final state for different intermediate processes normalised to the number of stopped  $K^-$  in the DC wall. The statistical and systematic errors are shown as well [11].

normalised to the total number of stopped antikaons. The fit results lead to the first measurements of the genuine 2NA-QF for the final state  $\Sigma^0 p$  in reactions of stopped  $K^-$  on targets of  $^{12}\text{C}$  and  $^{27}\text{Al}$ . This contribution is found to be only 9% of the total absorption cross-section. The last step of the analysis consists in the search of the  $ppK^-$  bound state produced in  $K^-$  interaction with nuclear targets, decaying into a  $\Sigma^0 p$  pair. The  $ppK^-$  are simulated similarly to the 2NA-QF process but sampling the mass of the  $ppK^-$  state with a Breit-Wigner distribution, rather than the Fermi momenta of the two nucleons in the initial state. The event kinematic is obtained by imposing the momentum conservation of the  $ppK^-$  residual nucleus system. Different values for the binding energy and width varying within  $15 - 75 \text{ MeV}/c^2$  and  $30 - 70 \text{ MeV}/c^2$  in steps of 15 and 20  $\text{MeV}/c^2$ , respectively, are tested. This range has been selected according to several theoretical predictions

present in literature and taking into account the experimental resolution. The global fit is repeated adding the  $ppK^-$ . The best fit ( $\chi^2/\text{ndf} = 0.807$ ) is obtained for a  $ppK^-$  candidate with a binding energy of  $45 \text{ MeV}/c^2$  and a width of  $30 \text{ MeV}/c^2$ , respectively. Figure 3 shows the results of the best fit for the  $\Sigma^0 p$  invariant mass and proton momentum distributions where the  $ppK^-$  bound state contribution is shown in green. The resulting yield normalised to the number of stopped

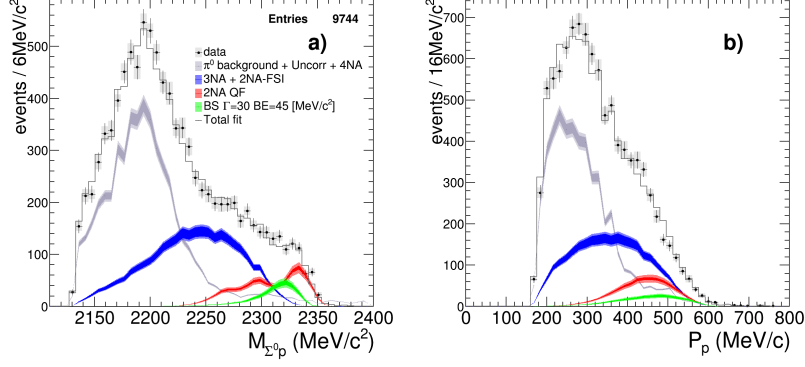


**Figure 3:** Experimental distributions of the  $\Sigma^0 p$  invariant mass,  $\cos(\theta_{\Sigma^0 p})$ ,  $\Sigma^0$  and proton momentum together with the results of the global fit including the  $ppK^-$ . The different contributions are labeled as in Figure 2 and the green histograms represent the  $ppK^-$  signal.

$K^-$  is  $ppK^-/K_{stop}^- = (0.044 \pm 0.009 \text{ stat}_{-0.005}^{+0.004} \text{ syst}) \times 10^{-2}$ . The F-test conducted to compare the simulation models with and without the  $ppK^-$  signal gave a significance of the result of only  $1\sigma$  for the  $ppK^-$  yield result [11]. This shows that although the measured spectra are compatible with the hypothesis of a contribution of a deeply bound state, the significance of the result is not sufficient to claim the discovery of this state.

## 5. Conclusions and perspectives

The broad experimental program of AMADEUS, dealing with the non-perturbative QCD in the strangeness sector, is supported by the quest for high precision and statistics measurements, able to set more stringent constraints on the existing theoretical models. We demonstrated the capabilities of the KLOE detector to perform high quality physics (taking advantage of the unique features of the DAΦNE factory) in the open sector of strangeness nuclear physics. Our investigations, presently spread on a wide spectrum of physical processes, represent the most ambitious and systematic effort in this field. In particular, in this report we have presented the analysis of the  $K^-$  absorption processes leading to the  $\Sigma^0 p$  state measured with the KLOE detector. It was shown that the full kinematics of this final state can be reconstructed and a global fit of the kinematic variables allows to pin down quantitatively the various contributing processes. Also, the possibility to accommodate a signal from a  $ppK^-$  bound state has been investigated. We proved the possibility to deliver very accurate and valuable results in the strangeness sector, in particular for what concerns the comprehension of the  $\bar{K}N$  potential, by studying all the possible channels following a  $K^-$  absorption on one or several nucleons, for very low momentum kaons. For the future, a dedicated AMADEUS setup, with dedicated gaseous and solid targets, where to enhance the fraction of stopped kaons, is under study.

## Acknowledgments

We thank all the KLOE Collaboration and the DAΦNE staff for the fruitful collaboration. Part of this work was supported by the European Community-Research Infrastructure Integrating Activity “Study of Strongly Interacting Matter” (HadronPhysics2, Grant Agreement No. 227431, and HadronPhysics3 (HP3) Contract No. 283286) under the EU Seventh Framework Programme.

## References

- [1] AMADEUS Letter of Intent,  
[http://www.lnf.infn.it/esperimenti/siddharta/LOI\\_AMADEUS\\_March2006.pdf](http://www.lnf.infn.it/esperimenti/siddharta/LOI_AMADEUS_March2006.pdf)
- [2] The AMADEUS collaboration, LNF preprint, LNF/9607/24(IR) (2007)
- [3] A. E. Nelson and D. B. Kaplan, Phys.Lett B192, 193 (1987).
- [4] T. Hyodo, D. Jido, Prog. Part. Nucl. Phys. 67 (2012) 55.
- [5] S. Wycech, Nucl. Phys. A 450, 399c (1986).
- [6] Y. Akaishi and T. Yamazaki, Phys. Rev. C 65, 044005 (2002).
- [7] T. Yamazaki et al., Phys. Rev. Lett. 104, 132502 (2010).
- [8] G. Agakishiev et al., Phys. Lett. C 85, 035203 (2012).
- [9] M. Agnello et al., Phys. Rev. Lett. 94, 919303 (2005).
- [10] T. Suzuki et al., Mod. Phys. Lett. A 23, 2520-2523 (2008).
- [11] O. Vazquez Doce et al., Phys.Lett. B 758, 134-139 (2016).
- [12] A. Gallo et al., Conf. Proc. C060626 (2006) 604.
- [13] F. Bossi et al. (KLOE coll.), Riv. Nuovo Cim. 31, 531-623 (2008).
- [14] M. Adinolfi et al., [KLOE Collaboration], Nucl. Inst. Meth. A 488, (2002) 51.
- [15] M. Adinolfi et al. [KLOE Collaboration], Nucl. Inst. Meth. A 482, (2002) 368.
- [16] K. Piscicchia et al., Nucl. Phys. A 954, 75-93 (2016)